Polymer 49 (2008) 3541–3553

Contents lists available at ScienceDirect

Polymer

journal homepage: www.elsevier.com/locate/polymer

A novel microstream injection molding method for thermotropic liquid crystalline polymers to promote mechanical isotropy: A matrixing microbeam X-ray study

D. Boles, M. Cakmak*, B. Yalcin

Polymer Engineering Department, University of Akron, Akron, OH 44325-0301, United States

ARTICLE INFO

Article history:
Received 29 April 2008
Received in revised form 4 June 2008
Accepted 4 June 2008
Available online 17 June 2008

Keywords:
Thermotropic liquid crystalline polymer
Injection molding
Microbeam X-ray diffraction

ABSTRACT

The effects of flow-altering inserts and mold cavity geometry on the mechanical properties of an injection molded liquid crystalline polymer were studied to produce parts with properties approaching macroscopically isotropic state. By inserting fine metal mesh barriers to the gates of the mold cavities, a large number of highly oriented microstreams are produced. After their creation these highly oriented streams of differing flow vectors intertwine and this texture remains reasonably intact even after substantial shearing and extension history imparted on them during ensuing flow into the cavity. This method is effective in the interior away from the skin regions formed under the shearing flow during injection. The local molecular orientation was determined using a matrixing microbeam WAXS technique that allows precision movement of the sample in the microbeam X-ray. Samples produced with the 1.0 mm^2 mesh showed large variations in the local symmetry axis with respect to the machine as measured by microbeam X-ray diffraction incrementally from the edge to the core of the parts. In comparison, samples with no mesh insert showed only gradual changes in the tilt angle (angle between local symmetry axis and flow direction). The modulus and tensile strengths of all samples with the 1.0 mm^2 mesh inserts were found to approach virtual global mechanical isotropy.

1. Introduction

The thermoplastic polymers are shaped by injection molding first by melting them in the screw extruders and subsequently pumping them through small channels where they experience complex thermal-deformation histories including substantial shearing before ending in a cold cavity and solidify. The polymer chains that are subjected to such thermo-mechanical treatment become oriented [1–4]. In such conditions, the thermotropic liquid crystalline polymers orient with ease as a result of their low melt viscosity and relatively long orientation relaxation times [5]. Hence, even the core regions of injection molded TLCP parts, where the chain relaxation is favorable due to prolonged exposure to higher temperatures, remain highly oriented after the solidification as observed by microbeam X-ray techniques [6,7].

Thermotropic LCPs tend to provide a high degree of strength and stiffness primarily in the direction in which their stiff chain axes are oriented. This is particularly significant when small mold gaps are utilized where high shearing is dominant [8,9]. The high strength, stiffness and anisotropy exhibited by these materials may be beneficial for some applications but may prove to be detrimental for others as they provide a "woody" texture to the finished parts. This texture with higher orientation in the flow direction (FD) leads to poorer mechanical properties in the transverse direction [10–19]. So the problem is to reduce this mechanical anisotropy through a processing scheme where the oriented polymer chain bunches are randomized while they are flowing into the cavity.

This reduction in orientation relaxation exhibited by TLCPs has also been observed in particle filled flexible polymers particularly when the particles are nano-sized and create large interfacial area between the polymer and solid particles [20,21]. Platelet type fillers not only easily orient in the flow field but also amplify shearing on the Nylon-6 polymer chains trapped between them. This leads to substantially enhanced the preferential orientation of Nylon-6 chains. As a result of great reduction of their orientation relaxation of polymer chains due to their proximity to the solid surfaces of the nanoparticles, the developed orientation substantially maintained after solidification. This behavior very much resembles the behavior of TLCPs.

There have been various techniques developed to influence the orientation behavior of the polymer chains during injection molding. This includes rotating mold surfaces developed at Dow Chemical Laboratories [22,23] to impose preferential orientation of chains in materials such as polystyrene in order to improve their mechanical

* Corresponding author.
E-mail address: cakmak@uakron.edu (M. Cakmak).

0032-3861/$ – see front matter © 2008 Elsevier Ltd. All rights reserved.
doi:10.1016/j.polymer.2008.06.016

properties. More recently [24,25] a process was introduced to the market in order to apply push–pull action to the solidifying polymer melt injected into the cavity. This results in increasing preferential orientation levels in the core of the molded parts and appears to be suitable for polymers with fast orientation relaxation character such as polyolefin and some engineering plastics. These techniques act to promote orientation development. Other than obvious control of molecular architecture, we have not found a good technique to reduce the orientation and thus mechanical anisotropy.

The control of orientation in injection molding of TLCPs is typically carried out by changing the mold cavity geometry. It was demonstrated that regions of converging cross-sectional area in injection molds tend to promote a high degree of orientation in the flow direction, creating large anisotropic properties. Diverging mold cavity regions, on the other hand, give rise to a molecular structure that is perpendicular to the flow direction in the sublayers or the core due to the melt deceleration associated with this type of flow. A flow into thinner cavities maximizes the shearing during solidification during flow and this results in substantial orientation in the flow direction. Only fan-type gating of injection molds has proven effective in producing orientation perpendicular to the injection direction due to the decelerating flow field the material experiences in these gate regions [26].

In this paper, we take entirely different approach: we use locally flow-altering mesh inserts placed at the entrances of the mold cavities that produce multiple streams during injection. The purpose of the introduction of the mesh inserts is to deliberately produce individual small streams that are highly oriented on the local scale and come out flowing in different directions beyond the flow-altering mesh. The objective is to promote *global isotropy* by intertwining of these small streams during the filling of the injection mold cavity. We have already shown this effect to be valid for capillary extruded TLCPs with porous inserts in the pathway of extrusion [27].

To test the viability of this method, we have varied the mold cavity geometry to assess the influence of these local shearing inserts. The flow-altering mesh cavity inserts are used especially to control the local flow behavior and the orientation in the core regions of the molded parts.

2. Experimental procedures

2.1. Material specification

The material used was an aromatic poly(ester-amide) with a chemical name of 1,4-benzenedicarboxylic acid. This polymer was made up of 6-(acetyloxy)-2-naphthalenecarboxylic acid and *N*-[4-(acetyloxy) phenyl] acetamide, commercially known as VECTRA B950RX, manufactured by Hoechst Celanese (now Ticona). This material was supplied in the form of reactor chips that were approximately twice the size of a typical polymer pellet. VECTRA B950RX has a melting point in the region of 280 °C, reported by the manufacturer, and the base resin had a molecular weight greater than 20,000. The TLCP was dried in a vacuum oven at 150 °C for a period of 24 h before being used in any experimentation.

The porous metal screens used for this study had a regular square mesh pattern as shown in Fig. 1. These screens were made up of many thin wires that were interwoven (but not connected at each juncture) to form the mesh pattern. The thin wires were solid stainless steel and the screens were manufactured by the Williams and Mettle Company. The mesh openings were square, with the dimensions given in Table 1.

2.2. Injection molding

The injection molding was carried out on a Newbury Imperial 40-ton reciprocating screw plastic injection molding machine, model H2-40RS. The machine was equipped with a special mold-supporting device.

The screen inserts were placed in the injection mold cavities to disrupt the flow patterns developed during processing. The insert placement is illustrated in Fig. 2.

VECTRA B950RX samples were prepared at a volumetric injection rate of 24.6 cm^3/s, mold temperature 15 °C, melt temperature 310 °C, injection pressure 7.5 MPa, and holding times 45–60 s. The injection molding barrel zone temperatures were kept at 275, 290 and 310 °C, from feed to nozzle.

2.3. Injection molding cavities

The mold cavities designed for the injection molding machine are shown in Fig. 3. The mold cavities and mold temperature controllers were fabricated to be used with an existing mold support unit attached to the injection molding machine. These cavities were machined from cold-rolled steel plates and were finish polished by hand to the required degree of smoothness.

Table 1

Screen designation	Mesh opening area (mm^2)
Mesh A	1
Mesh B	0.25

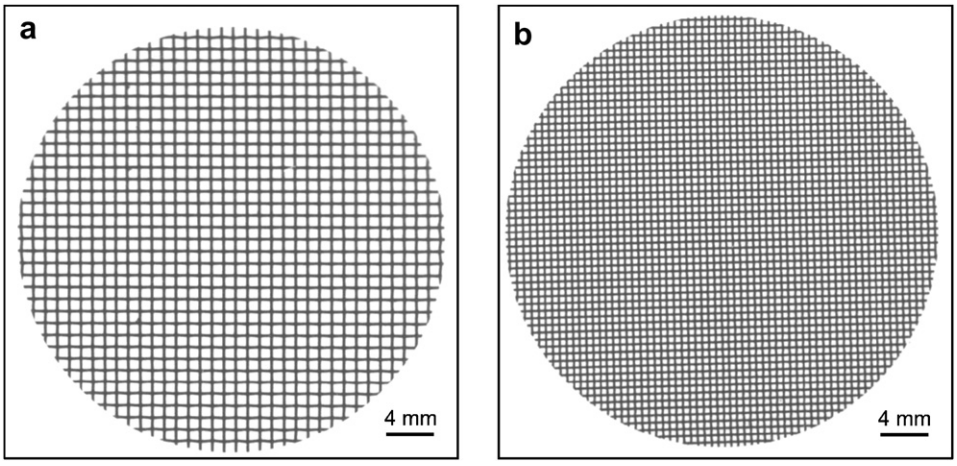

Fig. 1. Schematics of (a) mesh screen insert "A" with 1.0 mm^2 unit opening area and (b) mesh screen insert "B" with 0.25 mm^2 unit opening area.

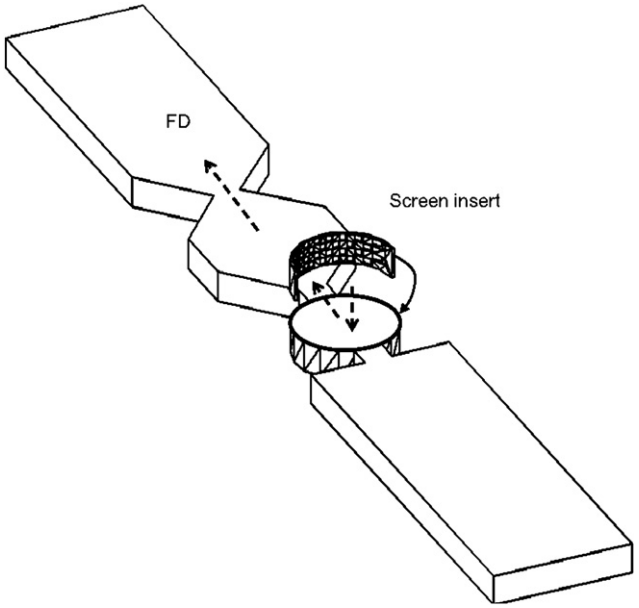

Fig. 2. Schematic showing the placement of the metal screen insert in the injection mold cavity.

Mold cavity 1 was drawn to scale and had a thickness of 4.0 mm. This cavity will be referred to as Mold 1 for future reference. This mold featured a rather complicated geometry and the significance of each region is explained in Fig. 3 (right). The cavity began with a large gate and inlet region (4.0 mm × 4.0 mm) which leads into the first diverging region followed by a short transition region. Next, the geometry changed to a converging region followed directly by another diverging region. Finally, the melt flowed into the region of the mold that formed the boundaries for the sample that was characterized and tested.

Mold 2 also had a thickness of 4.0 mm along with entrance and beginning regions identical to those of Mold 1, but the sample width was doubled. This double divergence scheme was developed in order to investigate whether this sequence can substantially erase the shearing/orientation history applied at the entrance region of the cavities.

2.4. Cutting procedures

In order to investigate the three-dimensional structural variations, the Leco VC-50 Low Speed Precision Diamond Saw was used for all cutting procedures. We elected to cut the samples in three cutting modes called "A"–"C" cuts which are graphically shown in Fig. 4. Procedure "A" produced thin samples (0.4 mm) that were cut in the ND–TD plane normal to the flow direction at seven specific regions of interest along the parts. Procedure "B" consisted of removing a thin section (0.4 mm) of the part along the center symmetry plane (FD–ND) normal to the TD. Procedure "C" was used to create a thin sample (0.4 mm) from the center of the part in the FD–TD plane halfway distance between the top and bottom surfaces.

A 4″ diameter diamond impregnated blade was used for the "A" cuts. This blade was approximately 0.3 mm in thickness. The "B" and "C" cuts were performed using a 5″ diameter diamond blade identical to the 4″ blade previously mentioned.

For the mechanical property tests, samples from Mold 2 were cut at 0°, 45°, and 90° to the flow direction using the procedure shown in Fig. 5.

2.5. Wide angle X-ray diffraction (WAXD)

The WAXD analysis was performed using a Rigaku Rotoflex unit with a 12 kW rotating anode generator. This machine was equipped with a special microbeam camera designed in our laboratory [7]. This camera allows a series of WAXD patterns to be taken at selected locations in the part without dismounting of the part. The diffraction patterns were produced using a 75 μm diameter collimated X-ray beam The X-ray beam was monochromatized with a nickel foil filter. The machine was operated at 40 kV and 150 mA.

Quantitative molecular chain orientation data was gathered using WAXD film patterns obtained using the micro camera. From the WAXD patterns, the azimuthal intensity profiles and the intensity profiles in the 2θ direction were obtained.

The degree of orientation in samples of uniaxial symmetry is commonly defined by means of Herman's orientation factor denoted by

$$f = \frac{[3\langle\cos^2\chi\rangle - 1]}{2} \tag{1}$$

where χ is the angle between the chain axis and the reference direction (e.g. fiber axis, flow direction, etc.). The value of $\langle\cos^2\chi\rangle$ was computed from the azimuthal angular distribution of WAXD intensity profile denoted by

$$\left\langle\cos^2\chi\right\rangle = \frac{\int_0^{\frac{\pi}{2}} I(\chi)\cos^2\chi\sin\chi\,d\chi}{\int_0^{\frac{\pi}{2}} I(\chi)\sin\chi\,d\chi} \tag{2}$$

where $I(\chi)$ is the digitized angular intensity profile from the WAXS diffraction pattern.

In the isotropic randomly oriented state $f = 0$; if the chain axis alignment is in the machine direction, $f = 1$; and if the alignment is perpendicular to the machine direction, $f = -0.5$ [4].

The azimuthal intensity profile data was used in the calculation of the orientation factor and the determination of the tilt angle of

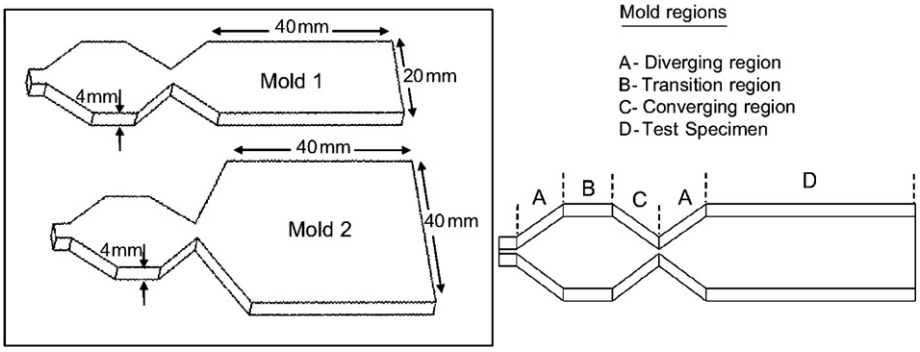

Fig. 3. Schematic of Mold 1 and Mold 2 and description of the mold regions.

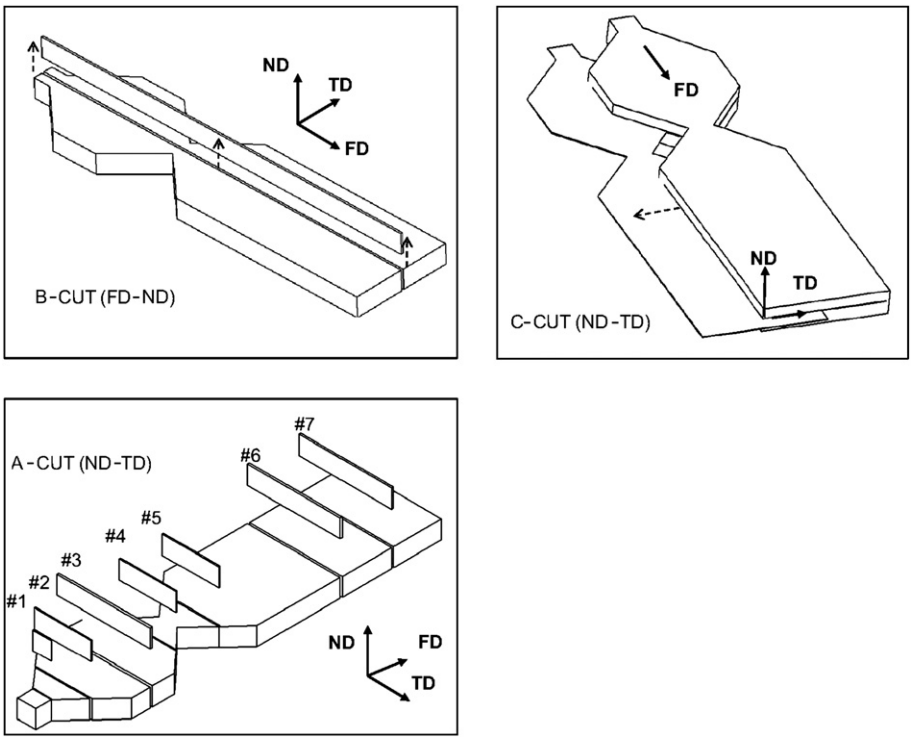

Fig. 4. Schematic of A-cut, B-cut and C-cut procedure (ND: normal direction, TD: transverse direction, FD: flow direction).

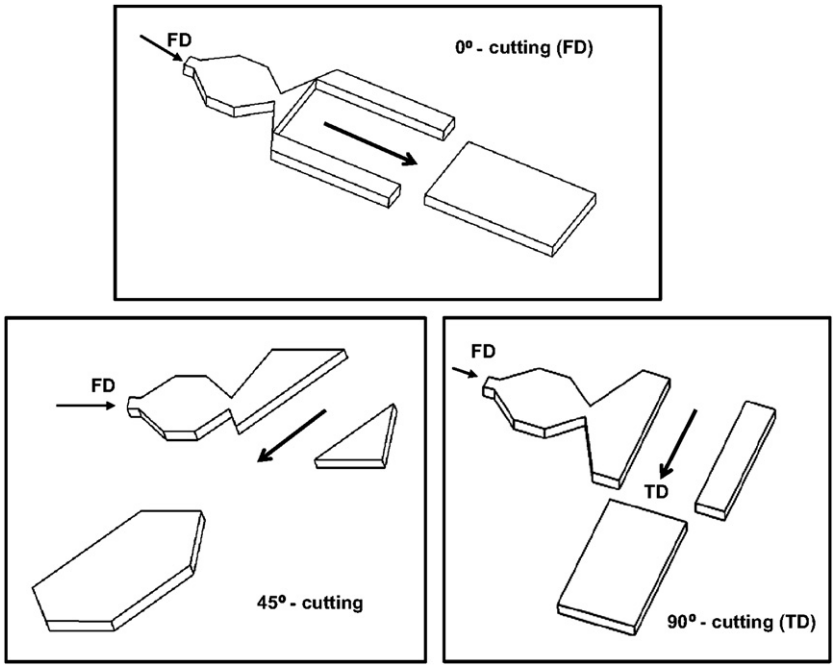

Fig. 5. Schematic of the cutting procedure used for Mold 2 in directional dependency of mechanical property tests. Angle values are with respect to the FD.

the orientation with respect to a reference direction. In this case we chose flow direction as the reference direction.

2.6. Digital image analysis

The intensity profiles from skin to core of the injection molded samples were collected for optical property detection. All images were smoothed using a median filter (whereby input data is replaced by the median of its neighbors) before data was collected.

2.7. UV–vis spectroscopy

A thin, highly oriented sample of 32 μm in thickness was taken from the skin region of an injection molded part and was scanned from a wavelength of 900 to 300 nm to determine the

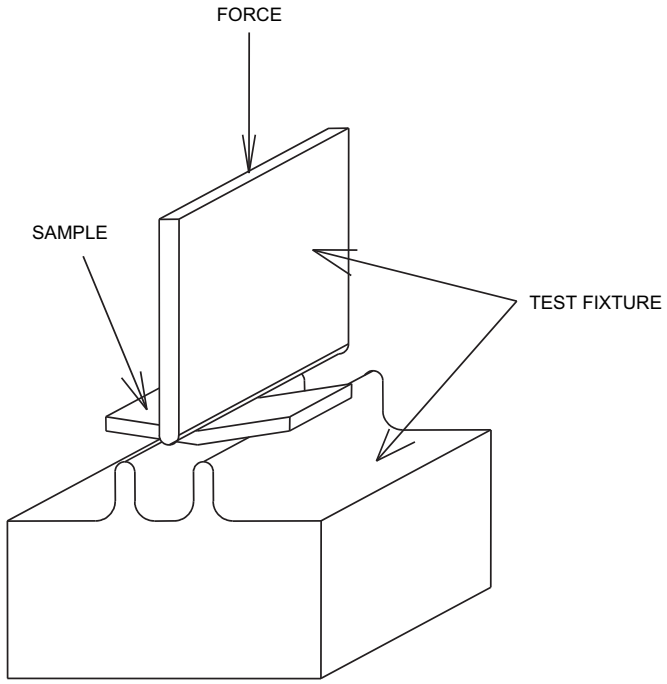

Fig. 6. Schematic of the test fixture used in conjunction with the T4024 testing machine for the three–point flexural testing.

transmittance peaks. These experiments were done using a Perkin Elmer model 559A Spectrophotometer at room temperature.

2.8. Three-point flexural testing

The three-point flexural bending tests were done using an Instron T4024 tensile testing machine in the flexural mode. The test fixture used for the flexural tests, in conjunction with the Instron machine, is shown in Fig. 6. The span between the lower point contacts was 25.0 mm. The T4204 was equipped with a 50 kN load cell. The tests were done with a cross-head speed of 5.0 mm/min. Four or five samples from each molding condition were tested.

2.9. Tensile testing

The tensile testing was done using the Instron T4024 tensile testing machine in the tensile mode. The sample gauge length, 15.0 mm, was used for all samples tested. The T4204 was equipped with a 50 kN load cell. The tests were done with a cross-head speed of 5.0 mm/min. Four or five samples from each molding condition were tested and the results were averaged.

3. Results and discussions

3.1. Optical anisotropy

TLCP materials readily orient in the flow fields of the injection molding process. In order to allow the TLCP material to enter the porous screen with a limited amount of orientation, the injection mold cavities were designed with a very large sprue region (diameter approximately 15.0 mm). The large sprue, which followed directly after the exit from the nozzle, allowed for a deceleration of the melt before it reached the cavity entrance. During this sprue filling, internal jetting was observed throughout the sprue region. This jetting was expected to help in the disorientation process by creating swirling layers in the TLCP melt before it entered the cavity.

As shown in Fig. 7, after the melt exited the porous screen, several small streams were produced. The sample produced with no insert showed no disruption in the flow pattern with little color variations in the core regions. The sample with the mesh "A" and the mesh "B" inserts, on the other hand, clearly showed these individual streams introduced to the melt. Due to the local large shearing and acceleration that takes place as a result of

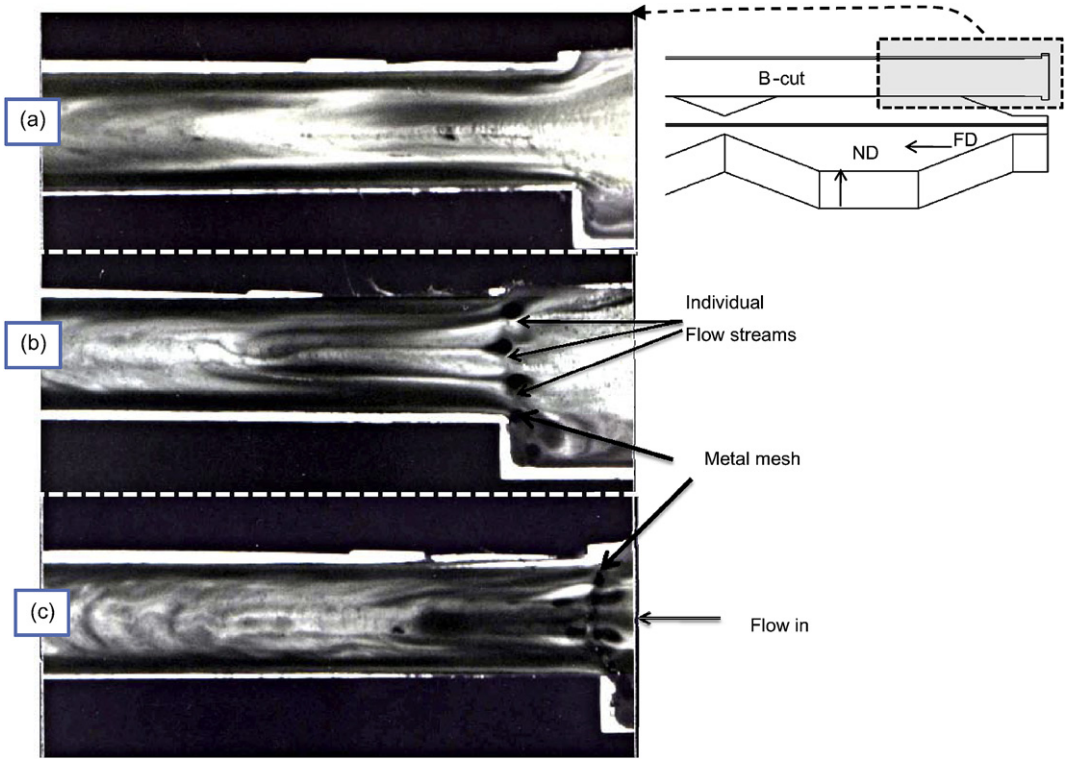

Fig. 7. Cross-sectional view of the samples cut with B cut in ND–FD plane in the boxed region (see inset) at the entrance of the cavity (a) no mesh, (b) Mesh B and (c) Mesh C.

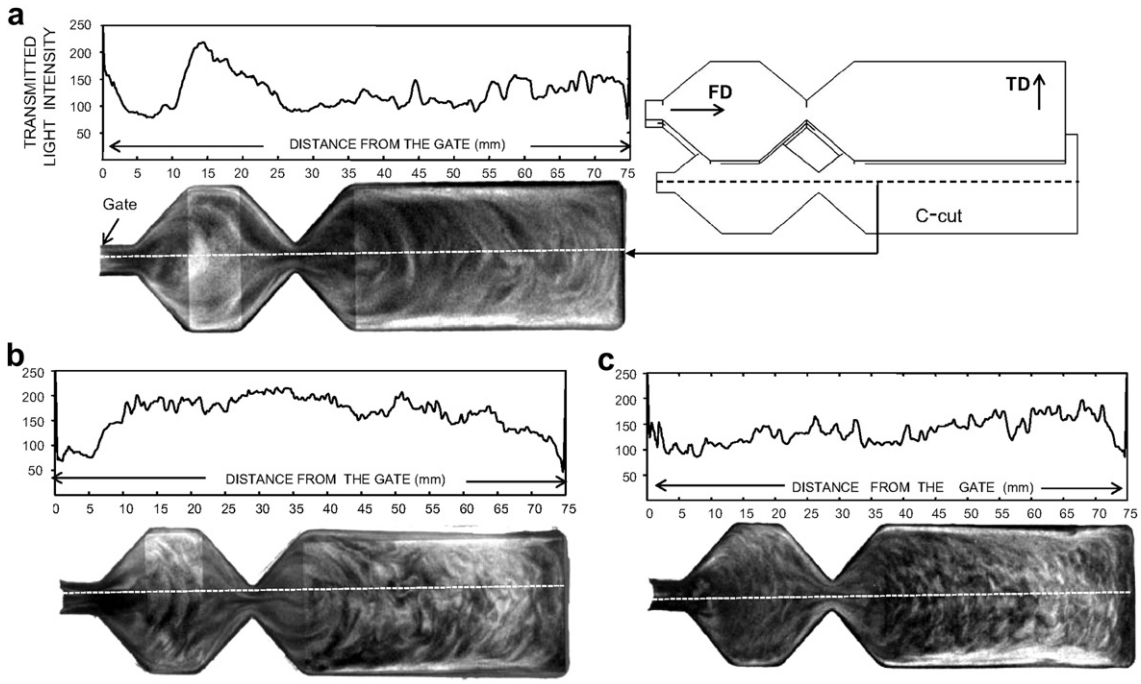

Fig. 8. Optical images of the planar "C" cuts of injection molded samples with (a) no insert, (b) a mesh "A" insert and (c) a mesh "B" insert along with their transmitted light intensity profiles in the flow direction along the centerline of the C cut. Shaded regions on the optical images are image enhanced for ease of observation.

convergence when the TLCP melt passes through the screen inserts, a large degree of local orientation is expected in the direction of flow.

The effect of the mesh inserts becomes very apparent by viewing the optical properties of the samples produced using Mold 1 in Fig. 8. This figure shows "C"-cut optical images of the samples injection molded in the absence (Fig. 8a) and presence of mesh inserts (Fig. 8b and c). The flow patterns were parabolic in all samples as expected from the fountain flow that takes place in injection molding. In the samples with the inserts, however, the parabolic form of the flow patterns was highly disrupted as evidenced by the dark–bright color fluctuations in areas between the flow lines. This was quantified and shown above each optical image by plotting the intensity profiles of the light which was transmitted through the samples along their center lines indicated on the images as short dashed lines. The sample with no insert showed relatively broad and fewer intensity fluctuations from the gate to the end of the sample. These fluctuations at the end of the sample are

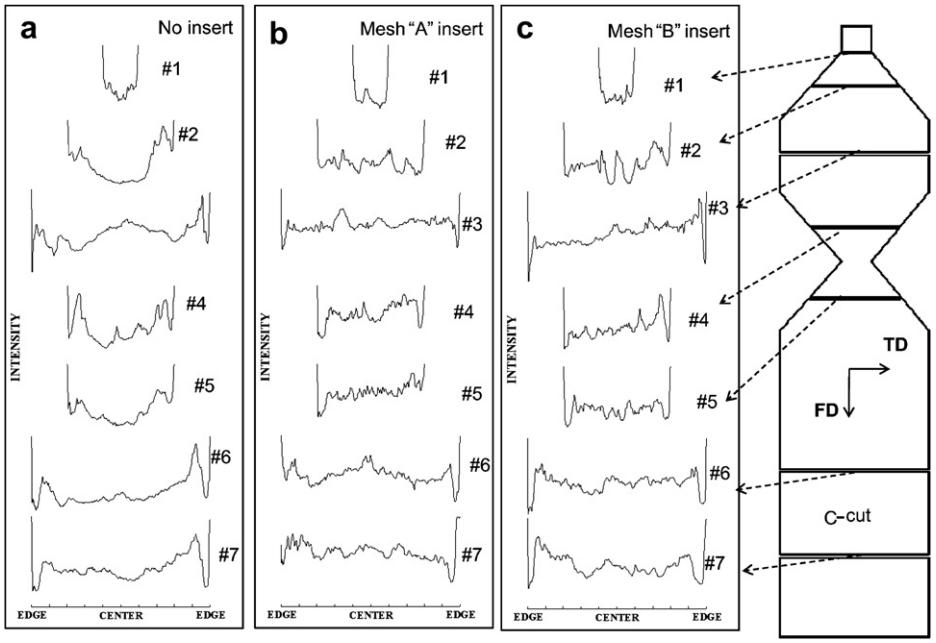

Fig. 9. Transmitted intensity profiles normal to the flow direction from the planar C-cut samples at the seven locations of interest (a) no insert, (b) mesh "A" insert and (c) mesh "B" insert. Short dashed lines on the right show the direction of intensity profiling.

due to end effects produced by the sudden stopping of the melt front at the end of the cavity filling. The transmitted light intensity profiles of the samples with the mesh "A" and mesh "B" inserts, on the other hand, showed more frequent and sharper intensity changes. Additionally, the flow patterns developed by the mesh insert in the early regions of the mold cavity remain throughout the sample even after the flow has passed through a converging–diverging region which normally tends to highly align (or re-orient) the molecular chains along the flow direction as a result of high shear flow.

Fig. 9 shows the transmitted light intensity profiles in the normal direction to the flow on the same C-cut samples of Fig. 8 at seven specified locations. As in the previous intensity plot along the centerline flow direction, the intensity profiles normal to the flow direction with the mesh inserts showed more frequent and sharp intensity fluctuations. The seven locations for the intensity profile studies were chosen because they fell in regions of the samples where the geometric changes occurred as described in Section 2.

Fig. 10 shows all three samples sectioned with the "B"-cutting procedure along with their transmitted intensity profiles along the flow direction. As previously observed for C-cut samples, the intensity changes are more frequent in the samples with the mesh "A" and mesh "B" inserts showing much finer texture development manifested in optical fluctuations. All of these observations were made for samples produced using Mold 1 cavity. The optical images and transmitted light intensity data of the samples produced using Mold 2 with a wider cavity were similar (not shown).

3.2. Matrixing microbeam X-ray studies

Having observed the substantial differences in the optical images of the samples produced with no inserts and those produced with the mesh inserts, we performed a very detailed WAXD study of the orientation level and tilt angle (local symmetry axis discerned by WAXS pattern and flow direction) developed on select samples at #2 and #6 positions (Fig. 4).

In order to assess the local orientation we used B (FD–ND) and C (FD–TD) cuts and selected the #2 position in the first chamber and #6 position (Fig. 4) in the second chamber and placed in a microbeam X-ray camera specifically developed for this study [7]. With built in precision X–Y stage this camera allows the acquisition of WAXS patterns using small X-ray beam. Fig. 11a illustrates a representative experiment obtained at #6 location from edge (#1) to core (#5) with X-ray beam directed in normal direction on a C-cut sample in the mid-plane. Since there were large number of WAXS patterns obtained for quantitative analysis these patterns are examples for indicated locations. For example near the side surface (#1, #2) locations fall inside a region where the material solidifies during the filling while undergoing substantial shearing. This leads to the local symmetry axes being oriented along the flow direction. In the interior regions (#3–#5) substantial redirections of local symmetry axes are observed. Fig. 11b illustrates the sampling with X-rays directed in the transverse direction at #6 location from skin to core. Though we also carried out the micro WAXS analysis in the samples cut in TD–ND plane, for the sake of brevity we are not presenting them here.

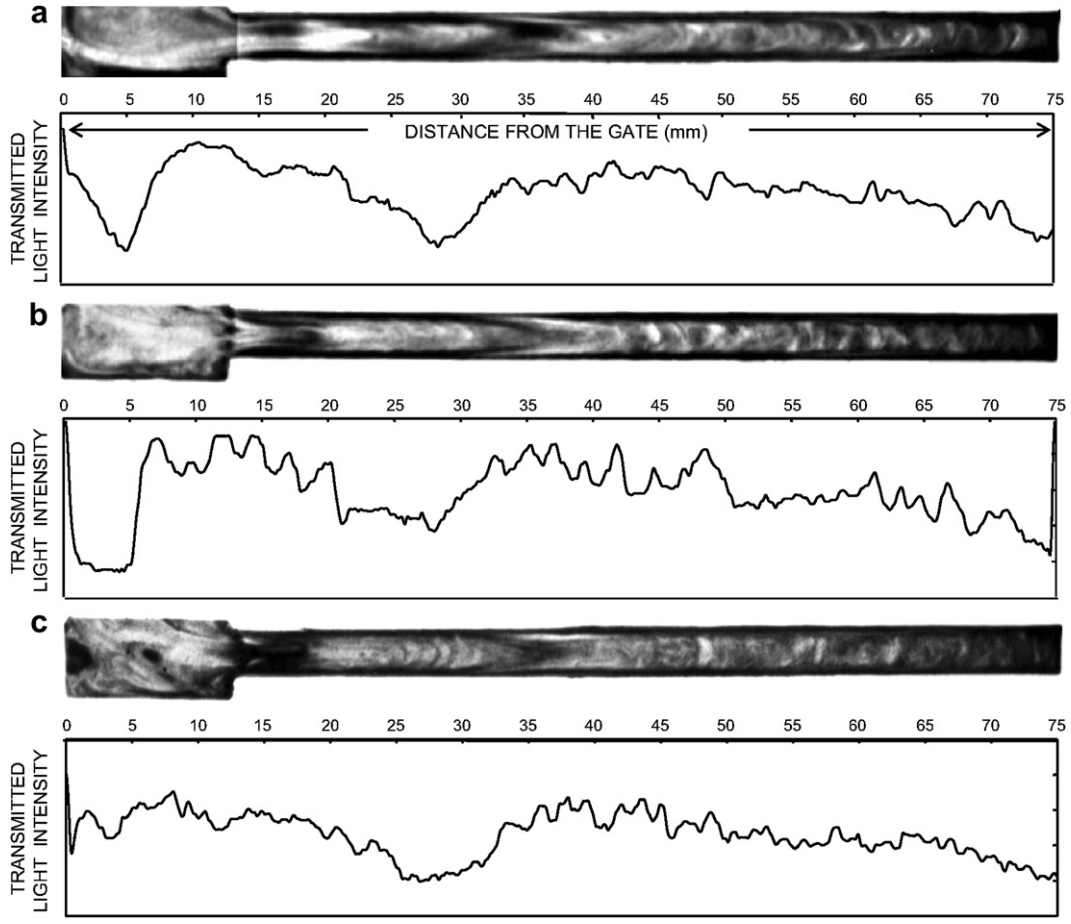

Fig. 10. Optical images of the B cuts of injection molded samples with (a) no insert, (b) a mesh "A" insert and (c) a mesh "B" insert along with their transmitted light intensity profiles in the flow direction along the centerline of the B cut.

Having obtained about 45 WAXS patterns from 0 to 10 mm from the edge at #2 location that is in the first chamber of our double chamber mold cavity, we analyzed the local symmetry axis directions with respect to flow direction (approx. tilt angle) and orientation factor of the primary equatorial peak representing chain–chain correlations with respect to local symmetry axis to obtain local orientation information. These two sets of data are shown in Fig. 12 for sample injection molded with no mesh insert at the gate. Near the skin (0–1.5 mm) the tilt angle is near zero and orientation factors are quite high. This represents the aforementioned shear region. Further inward towards the core deviations are observed and orientation levels become much milder. Insertion of fine mesh (Mesh B) for the same #2 location has pronounced effect on both orientation properties as illustrated in Fig. 13. Beyond a very thin skin (0–1 mm) large local variations in tilt angle and orientation factors are observed clearly attesting to the fact that mesh insertion does play significant role in shaping the morphology of the interior of the molded parts.

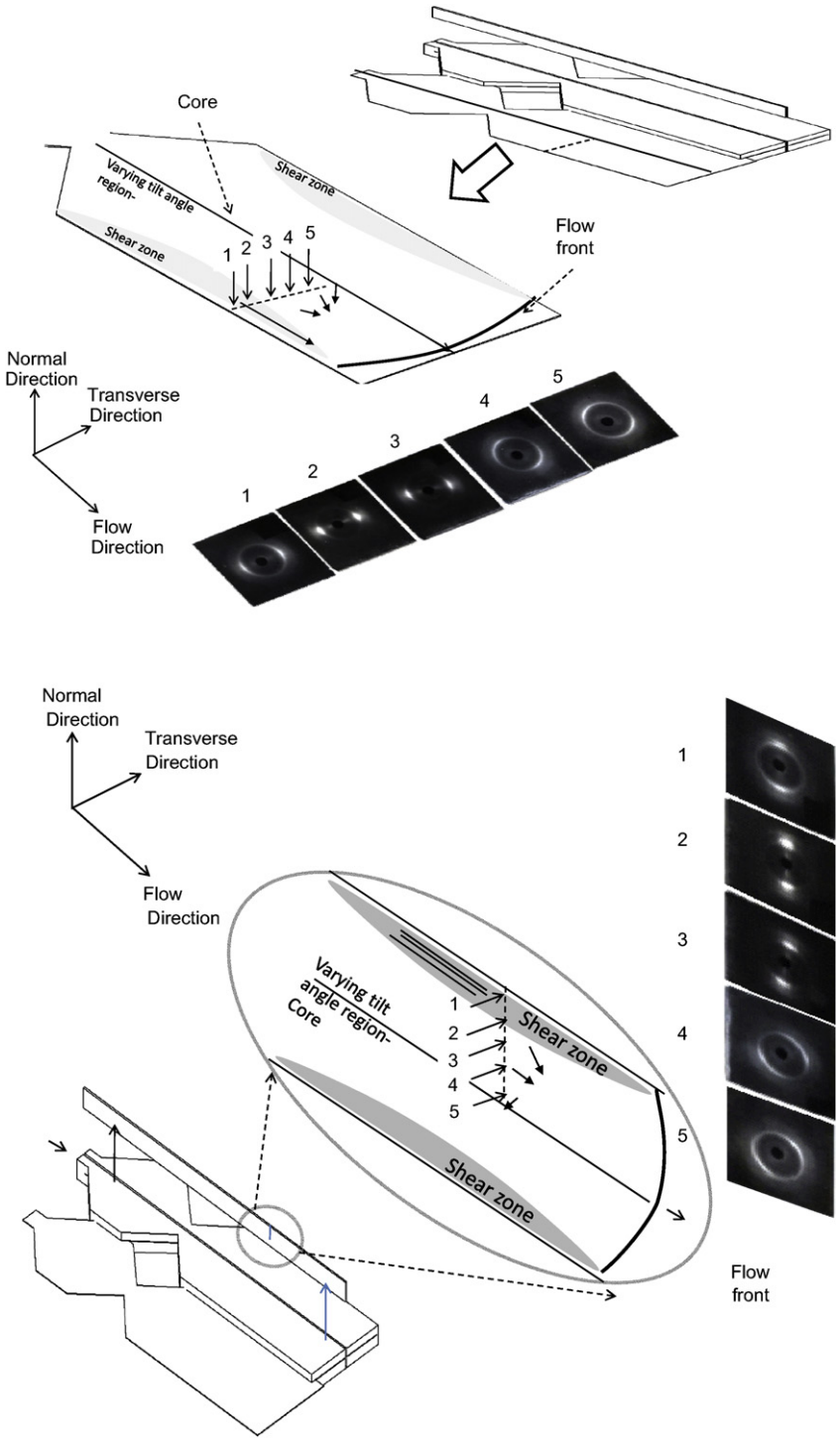

Fig. 11. WAXS patterns taken on (a) C-cut sample with X-rays directed in normal direction at designated locations and (b) B-cut sample with X-rays directed in normal direction at designated locations.

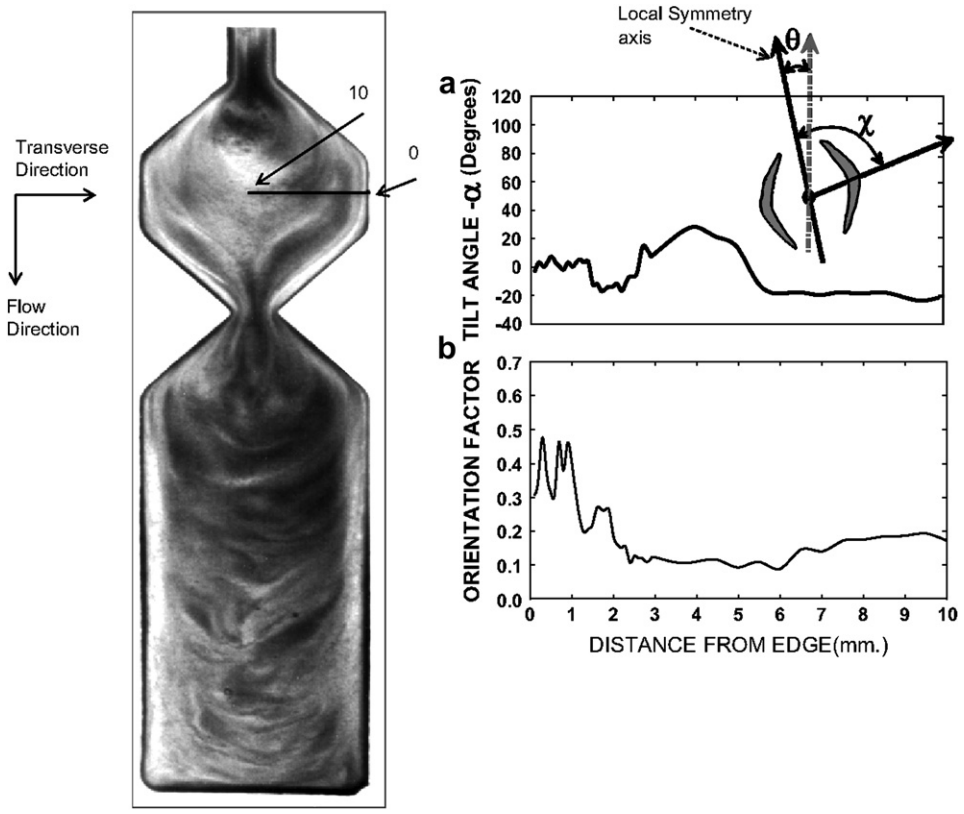

Fig. 12. At #2 position structure variation in width direction: (a) tilt angle and (b) orientation factor with respect to local symmetry axis for C-cut samples produced with no mesh at the gate. ϕ: local azimuthal angle; α: tilt angle.

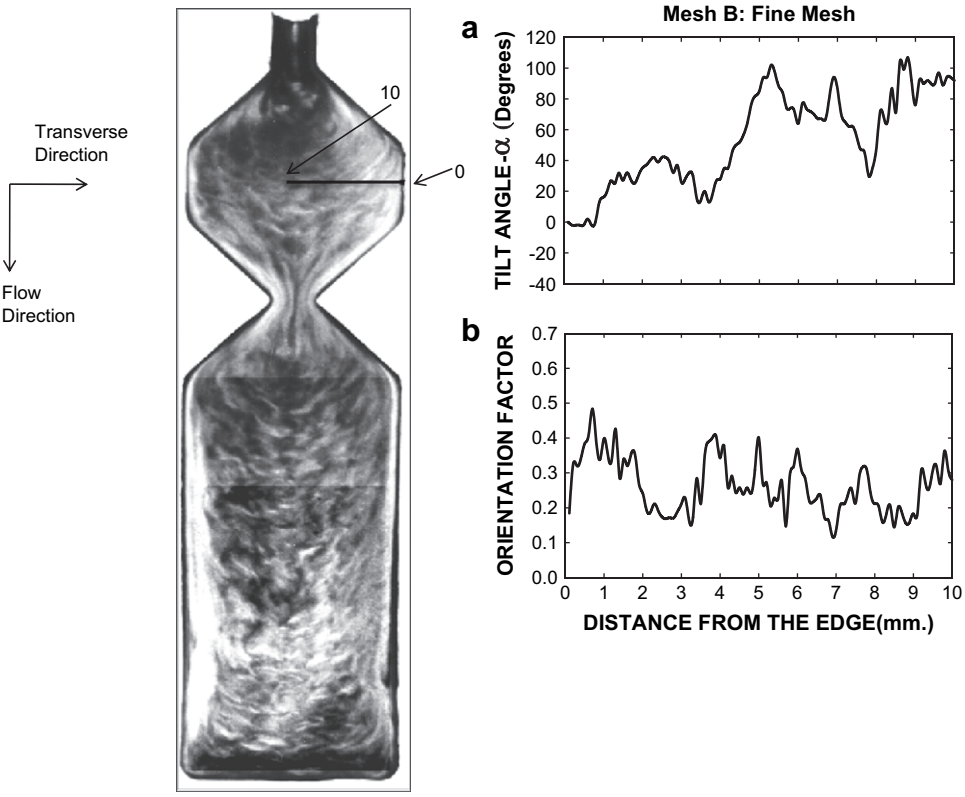

Fig. 13. At #2 position structure variation in width direction: (a) tilt angle and (b) orientation factor with respect to local symmetry axis for C-cut samples produced with Mesh B: fine mesh.

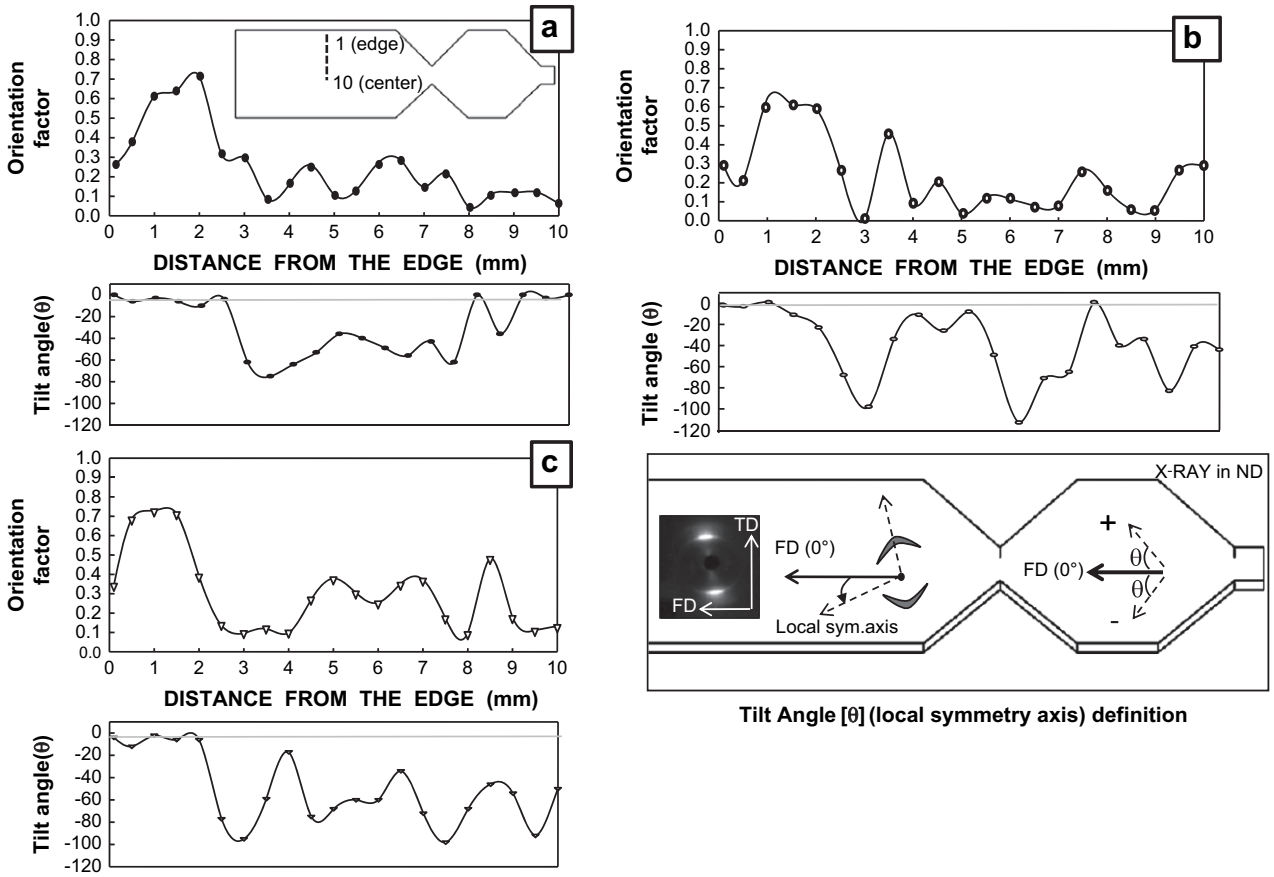

Fig. 14. Plots of orientation factor and tilt angle vs. distance from the edge of the C-cut samples at position #6 (a) no insert, (b) a mesh "A" insert and (c) a mesh "B" insert.

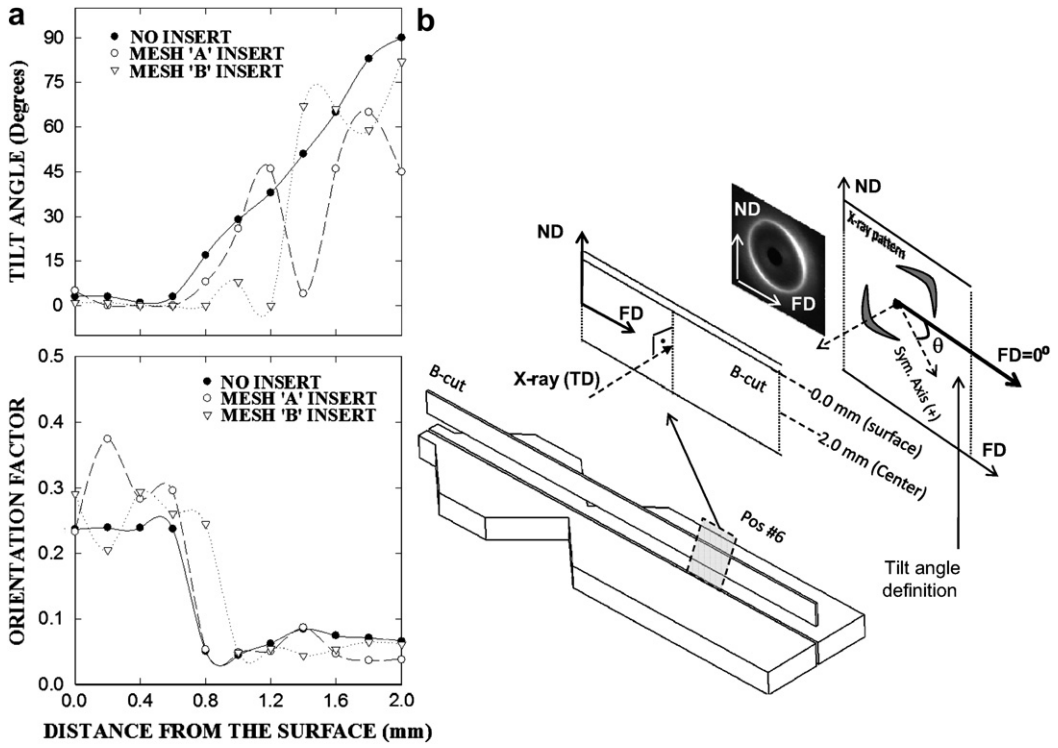

Fig. 15. Plots of orientation factor and tilt angle vs. distance from the surface to the core of the samples B-cut samples; #6 position (Mold 2 wider mold).

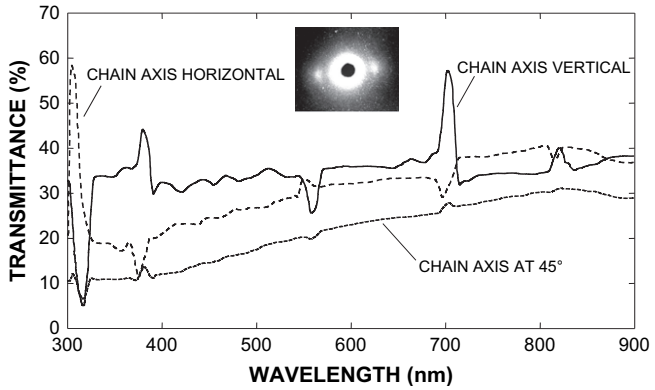

Fig. 16. UV–vis spectra of a sample removed from the skin of an injection molded sample with the chain axis in the horizontal, vertical and 45° directions.

3.2.1. Second chamber

The details of the orientation function and the tilt angle calculated from WAXD patterns scanned from edge to center in #6 position, the position where the failure from the mechanical testing would occur, are shown in Fig. 14. One can notice that all the three samples showed an increase of orientation factor from about 0.3 to about 0.7 near the edge (0–2.0 mm). As discussed earlier, the presence of mesh inserts does not seem to influence the orientation mechanism close to the surface regions where substantial shearing during solidification in injection stage takes place. This is the natural part of the nonisothermal injection molding process. As the hot melt contacts the surface it solidifies immediately and establishes melt–solid front at a given position that progresses towards the core of the sample during the injection stage. The area swept by this solid–liquid boundary is commonly called shear zone. At the boundary between the solid and melt substantial shearing takes place and this effectively dominates the local structure/texture development. As is evident from these data, we have little influence on the orientation behavior of this zone (Fig. 14a–c (0–3 mm thickness)). Further inward towards the core beyond about 3 mm from the edge, we notice that the samples with the mesh inserts show relatively large changes: from 0.7 (rather highly oriented) to 0.05 (rather low, approaching isotropic). From this point to the center, while the sample with no insert displays only three peaks ranging from 0.1 to 0.3, the samples with the mesh "A" and mesh "B" inserts display five peaks ranging from 0.12 to 0.46, and four peaks ranging from 0.1 to 0.49, respectively. To summarize, the orientation factors display large changes and more frequent fluctuations when the mesh inserts are present indicating large localized orientation fluctuations.

As for the tilt angles (defined in Fig. 14) of the main orientation axis, they remain relatively constant and aligned along the flow direction near the edge where the shear region is. Towards the interior, a sharp decrease at about 3.0 mm from the edge for all the samples is observed and this is indicating that the local orientations are tilted towards the mid-symmetry axis of the sample. From this point inward, however, the samples with the mesh inserts show several fluctuations in their molecular tilt angles, never reaching a constant value even close to the center of the sample. Especially, in the interior regions, not only the number of fluctuations is larger but also the degree they span between these fluctuations (from 0° to −120°) are higher than that produced with no mesh inserts (from 0° to −60°).

Similar WAXD experiments were performed with a wider mold, Mold 2, in order to investigate the mold geometry effect. The C cut showed similar results as in Mold 1. Therefore, we report the orientation effect from the surface to the core of the B-cut samples. In Fig. 15 (B cut), the sample with no insert displays a tilt angle that remains constant at 0° until about 0.6 mm from the surface which gradually rises to 90° towards the center of the sample. This was an expected result and related to the presence of fountain flow pattern which tangentially aligns the molecular chains along the parabolic flow gradually from 0° to 90°. At the surface of the sample, the molecular chains were aligned in the flow direction (tilt angle = 0°), and in the center of the part the molecular chains were aligned tangential to the end of the parabolic flow front (tilt angle = 90°). In the samples with the mesh inserts, on the other hand, the data does not wholly reflect the predictions of the fountain flow as the gradual change is replaced by random fluctuations showing that the inserts had a substantial effect on the flow field during mold filling.

As for the orientation factors, all three samples display very similar plots for the orientation factor in the B cut which indicates that although the mesh insert altered the tilt angle of the molecular chains, it had little effect on the degree of orientation of these chains. This is a positive effect since we do not want to sacrifice orientation levels that control the mechanical modulus and strength but only randomize the tilt angles to achieve mechanical isotropy.

In order to elucidate the variations of color at different layers in the cut specimens, a highly oriented and very thin film (thickness of 32 μm) of the TLCP was prepared from the skin layer of an injection molded part. The WAXD film pattern of this sample is shown in Fig. 16 along with its UV-vis spectra. The WAXD data clearly shows very high orientation along the major axis (flow direction). It is clear that there was a strong absorption band at 330 nm (approx. the blue range) which showed strong visible dichroism depending upon the direction of polarization. It is believed that this is responsible for the changes in color at different layers where orientation also varied. Since this linear relationship exists, it may be possible to approximate changes in the degree of orientation in a sample without the use of WAXD techniques. Nonlinearities in absorption due to the presence of gratings (for wavelength adjustment) and mirrors were verified (not shown) to be negligible and therefore not corrected.

From the optical photographs of the samples produced by the "C"-cutting procedure and the tilt angle information from WAXD data, it is clear that the flow fields of the samples with the mesh inserts deviate from the traditional fountain flow particularly at local level. The intensity profiles of the samples tend to show quite frequent fluctuations when the mesh inserts are present. The tilt angle (θ) of the orientation (local symmetry axis) shows very large and frequent changes, especially in the core regions. All of these findings support the development towards global isotropy in orientation. Also evident from the photographs, the unusual flow patterns developed by the mesh inserts were not erased even after the melt passed through a diverging region with a very narrow passage. This indicates that the mold cavity geometry had little effect if any on the orientation development in the core regions.

Next we investigate the role of inserts on the mechanical property development.

3.3. Mechanical properties

The directional dependency of the tensile and flexural properties are shown in Figs. 17 and 18, respectively. The tensile data for the samples with no insert shows a decrease in the maximum tensile stress, from 53 to 36 MPa. This behavior is the norm for standard injection molded LCP materials, due to their high degree of molecular anisotropy. The tensile stress values of the samples molded with the mesh "A" inserts, on the other hand, are remarkably constant ranging between 51 and 46 MPa independent of angle from the flow direction. The samples with the mesh "B" inserts showed a trend similar to those with the mesh "A" inserts, but

not to the same degree. For the mesh "B" samples, the tensile stress remained almost constant for the 0° and 45° directions, but decreased to some extent at 90°. It is important to note that this decrease was still less than that observed for the samples produced with no mesh insert. The plot of the tensile moduli in Fig. 17 shows a rather constant value ranging from 1.0 to 1.2 GPa, regardless of insert condition or angle from the flow direction. This may be due to the fact that the highly oriented skin regions provide the initial resistance to deformation which is similar for all samples regardless of the presence of the mesh inserts.

As for the flexural properties, the sample with no mesh exhibits higher flexural stress and higher anisotropy: the value decreases slightly from 167 to 148 MPa with increasing deviation from the flow direction. The addition of the mesh "A" inserts improves further the isotropy of the flexural stress values, but the values are slightly lower, at 140 MPa, than those of the samples with no mesh.

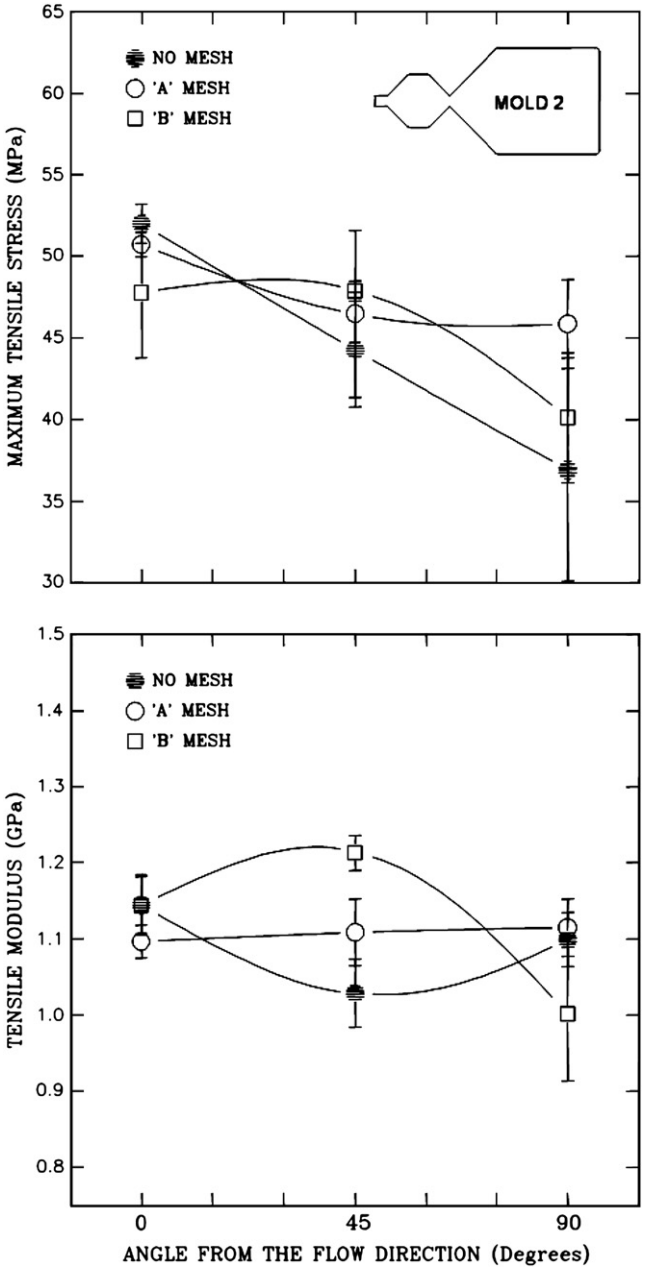

Fig. 17. Plots of the tensile properties vs. the angle from the flow direction for samples cut from Mold 2.

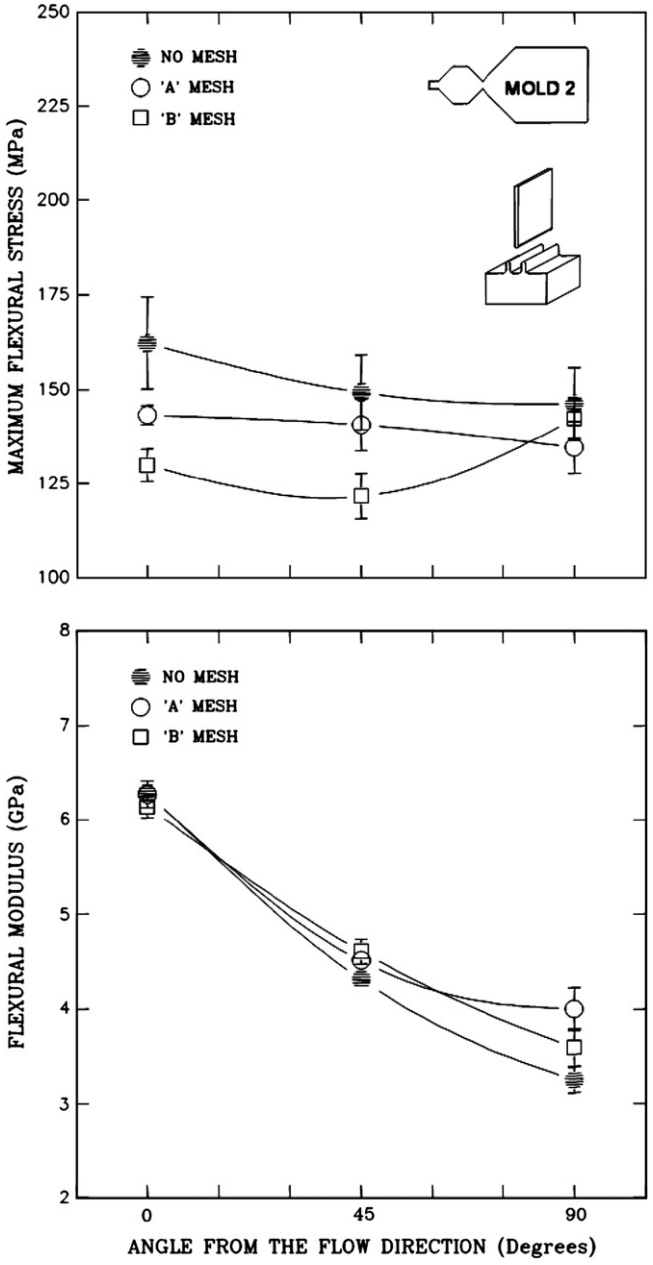

Fig. 18. Plots of the flexural properties vs. the angle from the flow direction for samples cut from Mold 2.

Samples with the mesh "B" insert showed lower (125 MPa), but isotropic, flexural stress values for both the 0° and the 45° directions, but the samples cut at 90° from the flow direction showed a dramatic increase in the maximum flexural stress (145 MPa), approaching the value of the no insert condition.

These tensile and flexural property results are in accord with the structural results and prove that at least the mechanical anisotropy in tensile and to certain extend in flex mode the properties approach isotropy.

4. Conclusions

The results in this study evidence that undesired mechanical and physical anisotropy originating from molecular anisotropy in injection molded TLCPs can be substantially alleviated simply by using metal mesh inserts placed at the gates of the standard molds.

The method is practical in achieving global isotropy by dividing the melt flow into many small streams through this metal mesh. These streams, in turn, intertwine with each other producing locally highly oriented streams that frequently change direction away from the skin regions of the injection molded part leading to structural and thus mechanical "macro" isotropy. The presence of mesh inserts was found to have little to no effect at the skins as these regions are formed under substantial shearing during injection that erases the prehistory given by the mesh inserts located upstream. Therefore, this method will be useful for cavities with larger thicknesses where this skin shearing effect is smaller.

References

[1] Wang YD, Cakmak M. Polymer 2001;42(9):4233–51.
[2] Kadota M, Cakmak M, Hamada H. Polymer 1999;40:3119.
[3] Ulcer Y, Cakmak M. Polymer 1997;38:2907.
[4] Hsiung CM, Cakmak M. J Appl Polym Sci 1993;47:125.
[5] Jin JI, Lee SH, Park HJ, Kim IJ. Polym J 1989;21:615.
[6] Hsiung CM, Tian J, Cakmak M. Int Polym Proc 1993;8:164.
[7] Hsiung CM, Cakmak M. Int Polym Proc 1993;8:255.
[8] Gogos CG, Huang CF, Schmidt LR. Polym Eng Sci 1986;26(20):1457–66.
[9] Heynderickx I, Paridaans F. Polymer 1993;34(19):4068–74.
[10] Blundell DJ. Polymer 1982;23:359.
[11] Whelen A, Goff JP. Developments in injection molding – 3. New York: Elsevier Applied Science Publishers; 1985.
[12] Wundr SL, Ramachandran S, Gochanour CR, Weinberg M. Macromolecules 1986;19:1696.
[13] Wissburn KF. J Rheol 1981;25:619.
[14] Wissburn KF. Br Polym J December 1980:163.
[15] Chung TS. J Polym Sci 1986;24:299.
[16] Cogswell NF. Br Polym J December 1980;170.
[17] Tuttle JR, Bartony Jr HE, Lenz RW. Polym Eng Sci 1987;27:1156.
[18] Rendon S, Burghardt WR, Bubeck RA, Thomas LS, Hart B. Polymer 2005; 46(23):10202–13.
[19] Rendon S, Bubeck R, Thomas LS, Burghardt WR, Hexemer A, Fischer DA. J Appl Polym Sci 2007;106(4):2502–14.
[20] Yalcin B, Cakmak M. Polymer 2004;45(8):2691–710.
[21] Yalcin B, Valladares D, Cakmak M. Polymer 2003;44(22):6913–25.
[22] Saunders FL, Cleereman KJ. SPE J 1969;25(9):44–8. 87.
[23] Saunders FL, Cleereman KJ. SPE Antec Tech Pap 1969;15:443–7.
[24] Ogbonna CI, Kalay G, Allan PS, Bevis MJ. J Appl Polym Sci 1995;58(11): 2131–5.
[25] Poomalai P. Popular Plast Packag 2005;50(4):79–82.
[26] Weng T, Hiltner A, Baer E. J Mater Sci 1986;20:744.
[27] Boles D, Cakmak M, Yalcin B. Polym Eng Sci, submitted for publication.